Bond between steel reinforcement bars and Electric Arc Furnace slag concrete

Flora Faleschini[1,*], Amaia Santamaria[2], Mariano Angelo Zanini[1], José-Tomás San José[2], Carlo Pellegrino[1]

[1] *Department of Civil, Environmental and Architectural Engineering, University of Padova, via F. Marzolo 9, 35131, Padova, Italy.*

[2] *Mining, Metallurgical and Materials Science Department, University of Basque Country, Alameda de Urquijo s/n, 48013 Bilbao, Spain*

* Corresponding author: flora.faleschini@dicea.unipd.it, Tel/Fax. +39 0498275585

ABSTRACT: This paper deals with the study of bond between steel reinforcement bars and recycled aggregate concrete, including Electric Arc Furnace (*EAF*) slag as full replacement of natural coarse aggregates. Pull-out tests according to RILEM standard were carried out on specimens made with six concrete mixtures, characterized by different w/c ratios and aggregates' types. Two types of steel reinforcement were used: plain and ribbed bars, to observe also the influence of steel roughness. Experimental bond-slip relationships were analyzed, and the results allow to state that similar mechanisms of bond are developed both in the reference concrete or when EAF slag is used as recycled coarse aggregate. Significant bond strength enhancement is observed in concretes with low w/c ratio, when EAF slag is used as recycled aggregate. Experimental results in terms of bond strength were also compared to analytical predictions, obtained using empirical formulations.

Keywords: Bond, EAF slag, Pull-out test, Recycled Aggregate Concrete, Splitting.

1. Introduction

Since the last two decades, many efforts have been made to develop novel concretes with reduced embodied energy, using recycled materials in place of ordinary binders and natural aggregates. Between the various possibilities for achieving this goal, many researchers have paid their attention on slag coming from metallurgical industry. According to local availability, research groups from Central Europe mainly studied Blast Furnace and Basic Oxygen Furnace slags potential use [1-3]. Conversely, in Southern Europe, Electric Arc Furnace (*EAF*) slag is more abundant, leading to a significant literature development about this material [4-8].

Previous studies already demonstrated that some properties of hardened concretes including EAF slag as coarse recycled aggregate are typically enhanced, if compared to corresponding conventional mixes with Natural Aggregates (*NA*s) only [9-11]. Particularly, *EAF* slag stiffness, morphology, shape, texture and chemical compounds are the reasons for its good performance as aggregate, and make it suitable for use in High Performances Concrete (*HPC*) also [11]. Durability tests performed on *EAF* concretes revealed that, in most cases, results are at least similar to the ones obtained with *NA* concrete [6,10,12-13], and in some cases also better, as in the case of chloride exposure [11]. Concerning fresh concretes properties, typically poorer workability was obtained by *EAF* mixtures, even though Water Reducing Admixture (*WRA*) can be added in the mixtures to achieve the required consistency.

In spite of the lack of standards about the use of *EAF* slag in cement-based materials, the above results encouraged some concrete producers to start using this material in mass applications, especially in gravity structures, where *EAF* concrete high density results is an advantage. Some real experiences confirmed the good results obtained at the lab-scale [14], pushing the research community to continue working for *EAF* slag standardization. In this context, a research group with several European partners from the University of Thessaloniki (Greece), Padova (Italy), Burgos and Basque Country (Spain) was created, aiming to study this topic.

Concerning the use of *EAF* slag for producing structural concrete, few works have been already done to test real scale elements: Pellegrino and Faleschini [15] analyzed the structural behavior of Reinforced Concrete (*RC)* beams under four point bending tests. Flexural behavior was critically analyzed, and the results obtained with *EAF* slag were compared with conventional concrete members, made with the same reinforcement. *EAF* concrete beams displayed higher ultimate capacity and reduced ductility, both for bending and shear failures. Kim et al [16] studied instead the behavior of spirally confined columns made with *EAF* concrete: experimental results revealed at least similar ductility compared to conventional specimens.

Up to now, there are still a lot of parameters that should be investigated to understand the structural behavior of this type of concrete. Bond between *EAF* concrete and steel reinforcement has not been analyzed in literature yet, and thus this research work aims to fulfill this gap. Bond strength is indeed one of the most important parameters in *RC* elements design, both at the ultimate and serviceability limit state. Its study is considered fundamental to verify that the same criteria used for *NA* can be adopted for *EAF* concrete members also. Pull-out tests were carried out on several specimens characterized by three aggregates' types and two w/c ratios, aiming to study both ordinary and (relatively) high strength concretes bond stress-slip relationships, with smooth and ribbed steel bars. All the other parameters that can influence bond behavior were kept constant. Even though it is well recognized that classical pull-out tests do not satisfactorily represents the same boundary conditions and stress states occurring in field structures, it has been chosen as the most convenient and simple test method to achieve an overall estimation of slag use effects on bond.

2. Background about steel-concrete bond

Bond is one of the most important properties of *RC* structures, and it refers to all the mechanisms allowing axial forces transmission from steel reinforcement to the surrounding concrete. An extensive literature exists about this problem [17-25], aiming to study the effects of various parameters, i.e. concrete quality, rebar diameter, concrete cover, confinement, fibers addition, etc. on the overall bond stress-slip behavior. Recently some experimental works were carried out also about bond between Recycled Aggregate Concrete (*RAC*) and steel reinforcement [26-29], but none of them used *EAF* slag as recycled aggregate.

Due to transmission mechanisms (namely chemical adhesion, friction and bearing of the ribs), the force acting on a reinforcing bar changes along its length, as well as the stresses in the concrete interface (embedded length). A relative displacement (slip) between steel and concrete occurs when steel differs from concrete strain. Bond stress can be defined as the equivalent shear stress acting on the interface between steel and concrete, i.e. as the rate of change of the force along the steel rebar, divided by the nominal area of bar surface over which that force change takes place [30]. Eq. 1 defines the bond stress:

$$f_b = (\Delta\sigma_s \cdot A_s)/(\pi \cdot \phi \cdot l_b) \qquad (1)$$

where f_b is the average bond stress over length l_b, $\Delta\sigma_s$ is the change of the stress in the bar over length l_b, A_s is the cross section area of the bar, ϕ is the nominal diameter of the bar and l_b is the bond length over which $\Delta\sigma_s$ takes place, i.e. the embedded length. The apparent simplicity of Eq. 1 relies in the fact that the above definition for bond stress is simplified and slightly inaccurate, due to the presence of the ribs on the majority of steel rebars currently employed for *RC* structures, which are used to increase bond resistance.

Concerning the test methods used for bond assessment, the pull-out test is the most used [31]: it allows to draw bond stress-slip curves and thus estimate the main characteristics of the bond stress–slip evolution. Many experimental works were based on this method [32-34], because it clearly represents the concept of anchoring a bar, through the use of economical specimens, and it provides a direct bond measure. However, some objections can be made to this type of test: test-setup places concrete in compression and bar in tension, a situation which is not common in the practice. Accordingly, the average measured bond is overestimated due to the absence of concrete transverse cracking. Additionally, bursting forces are generated due to the presence of ribs, which tend to split concrete cover. For this reason, two principal failure modes are possible, and they depend on geometrical parameters (e.g. concrete cover) and stress state (e.g. confinement): pull-out and splitting failures. The former occurs when concrete cover is large or high confinement reinforcement is present, and it displays concrete shearing across the tops of the ribs. When concrete cover is low, splitting failure occurs instead, and it is characterized by lower value of bond strength and thus is more critical for *RC* structures design. It is worth noting that other bond tests may be used, which can more properly represent the stress state of real design situation than the pull-out one. An alternative is given by the beam end test [35], which certainly provides better estimate of bond strength due to its similarity with structural flexural elements, but it is more complex and expensive than the classical pull-out.

3. Experimental program

3.1 Materials

Six concrete mixes were prepared to manufacture the specimens, varying w/c ratios and aggregates type. An ordinary Portland cement type I 52.5R class (with early age strength gain) was used for all the mixtures: cement included 90% of Portland clinker, 5% of calcium carbonate powder fines and 5% of gypsum. Water

was taken from the urban supply system of the city of Padova (Italy), and did not contain any undesirable compounds that could affect the quality of the concretes. A commercial *WRA* was used to allow the concretes to achieve the desired workability (S4 consistency class). River sand was used as fine natural aggregate in all the mixes, whereas three types of coarse aggregates were used: natural gravel aggregates with roundish shape, crushed natural limestone and *EAF* slag. Natural aggregates have typically a roundish shape in Italy, whereas *EAF* slag is very sharp and angular, thus it is considered more reliable to compare it to crushed aggregates. Hence the choice of using both roundish and crushed *NA*s allows to evaluate the influence of aggregates shape (regular vs. irregular) and origin (natural vs. EAF slag) on the bond stress-slip characteristics separately.
Physical properties of the aggregates are listed in Table 1. Concerning *EAF* slag chemical composition, it is mainly constituted by iron (Fe_2O_3 34.4%), calcium (CaO 30.3%), silicon (SiO_2 14.6%) and aluminum oxides (Al_2O_3 10.2%): a more detailed characterization of this slag can be found in a previous work of some of the authors [36]. It should be noted that the slag was previously stabilized via a pre-treatment, which included an outdoor weathering of at least 90 days and some daily wetting/drying cycles at the producer facility, to prevent potential expansive phenomena due to the hydration of free lime and magnesia. This operation was already demonstrated to be effective in this regard [4, 6, 10-11, 13].

Table 1. Physical properties of the aggregates.

	Coarse Aggregates			Fine Aggregates
	NA roundish	*NA* crushed	*EAF* slag	*NA* sand
Size (mm)	4-16	4-16	4-16	0-4
Bulk density (kg/m^3)	2701	2850	3854	2704
Water Absorption (%)	1.04	1.24	0.904	1.18

Concrete mixture details are listed in Table 2: two main parameters were varied, the w/c ratio and the aggregate type. In order to achieve two different strength targets, three mixes were manufactured with a low w/c ratio (0.45) and high cement dosage (400 kg/m^3), and the remaining three with a high w/c ratio (0.6) and a low cement content (300 kg/m^3). The same water content was maintained in all the specimens. An increase in *WRA* dosage was necessary for the mixtures including both *EAF* slag and crushed aggregates to achieve the required workability. Additionally, a slight variation in mixture proportions was necessary to take into account the different shape of roundish and irregular aggregates: hence, a slight increase in sand content was used for crushed and *EAF* slag aggregates' concretes.

Table 2. Mixture details (per m^3).

	*NAT*300	*NAT*400	*CRU*300	*CRU*400	*EAF*300	*EAF*400
Cement (kg)	300	400	300	400	300	400
Water (kg)	180	180	180	180	180	180
w/c	0.6	0.45	0.6	0.45	0.6	0.45
NA river (kg)	1039	987	-	-	-	-
NA crushed (kg)	-	-	908	863	-	-
EAF slag (kg)	-	-	-	-	1202	1156
NA river sand (kg)	851	808	1064	986	1082	991
WRA (kg)	0.6	2.8	2.1	4.0	1.2	4.0

The same mixing procedure was used for all the mixtures: dried aggregates were mixed for 1 minute; then cement and 2/3 of the total water were added and mixed for 3 minutes; concrete was left resting for 3 minutes; then the remaining 1/3 of water and the *WRA* admixture were added and the mixing procedure continued for 2 minutes. After mixing, fresh concrete workability was evaluated through the Abrams cone test, obtaining for all the samples a *S4* consistency class. Twelve cylindrical specimens with h x d = 200 x 100 mm were casted per each mix to evaluate compressive, tensile splitting strength and elastic modulus, according to the European standards of the *EN* 12390 series, at 7 and 28 days of ageing. Additionally, six cubic specimens (with 160 mm side) per each mix were manufactured for pull out tests. All the cylindrical and pull out specimens were demolded after one day; then they were cured in controlled humidity and temperature conditions (T= 20 ± 2°C; $RH \geq$ 95%), until time of testing.
Two different types of steel rebars were used to perform pull-out tests: plain and ribbed bars, both with a nominal diameter equal to 16 mm, and a nominal tensile strength of 500 MPa. The clear distance between the lugs in the ribbed bars was about 10 mm, measured at the lug mid-height. The choice of using smooth bars was governed by the necessity to analyze separately the aggregates influence on chemical adhesion mechanism. Specimens with ribbed bars were used instead to analyze in detail the mechanism of ribs bearing in bond strength development.

3.2 Pull-out test setup

Pull-out specimens were casted with the bar horizontal, being the casting direction perpendicular to the longitudinal axis of the bar. Cubes' side (160 mm) was 10 times the diameter of the bar (16 mm), and the embedded length (80 mm) was 5 times the diameter of the bar, following *RILEM* guidelines [31]. A plastic sleeve was used to limit the non-adherent zone (80 mm), situated at the loading face.
Tests were carried out at 28 days of ageing: the test setup is shown in Figure 1. A servo-hydraulic universal testing machine with a capacity of 600 kN was used to perform the test, and displacement-control was applied to capture the post-peak behavior. Load was applied at a rate of 0.3 mm/min and measured with the electronic load cell of the testing machine. The upper surface of the cube was restrained by a stiff 15 mm steel plate, with a hole of 32 mm diameter in the center. Between the specimen and the plate, a thin layer of rubber of 160x160x5 mm and another steel sheet of 160x160x5 mm were placed, to ensure that a uniform contact was realized and to minimize friction effects. The unloaded end slip was measured with a variable differential transducers (*LVDT*), with a precision of 0.001 mm (Figure 1 - *LVDT* 1). Two further *LVDTs* with the same precision were used during the test: one was placed onto the top surface of the specimen, and one onto the bottom (Figure 1 – *LVDT* 2 and 3), to check that no additional relative displacements affect the measure. An automatic data acquisition system was used to record the data. Six specimens for each concrete type were tested, being two sets of three nominally identical specimens, one with plain and one with ribbed bars. The test was stopped when failure occur for splitting of the surrounding concrete or for pull-out.

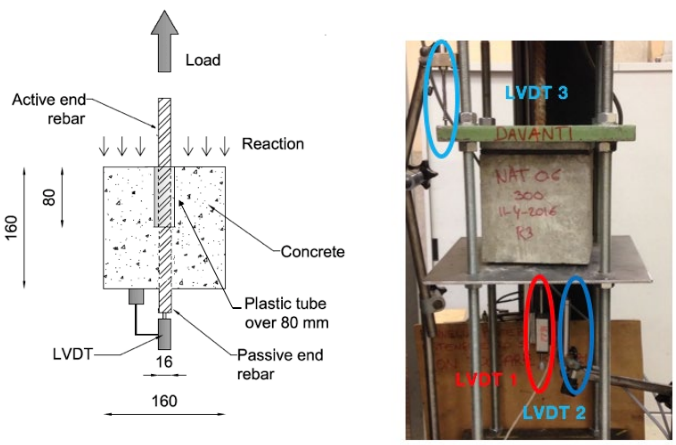

Figure 1. Setup for pull-out test.

4. Results and discussions

4.1 Concretes fresh and mechanical properties

The concretes produced in this work displayed a good workability, with a measured slump belonging to the *S4* class, being about 200 ± 5 mm, evaluated through the Abrams cone method. In all the cases the addition of the *WRA* admixture allowed to reach the required consistency, even if it is worth to note that when irregular aggregates were used (both *NA* and *EAF* slag), a remarkable increase of its content was necessary. Fresh density increases when *EAF* slag aggregate is used, respectively of +13.6% and +19.6% than in *NAT* for w/c 0.6 and 0.45, being proportional to the higher specific weight of this type of aggregate. The same occurs for the crushed *NAs* (+3.8% and + 2.7% for w/c 0.6 and 0.45), that in this case have a slightly higher specific weight than the natural roundish ones. Table 3 lists the fresh and hardened concrete properties together: results refer to the average of three specimens for each analyzed mechanical property.

Concerning compressive strength, for all the concretes produced with high w/c ratio, the failure was governed by the cementitious matrix low quality, regardless the aggregates type. As expected, no significant compressive strength differences were displayed between *NAT*300, *CRU3*00 and *EAF*300 mixtures. Conversely, in the concretes produced with low w/c ratio and high cement dosage, the influence of the aggregate type was relevant. Mixes produced with irregular shape aggregates were characterized by a strength gain of + 17.5% and + 30.7%, respectively in case of crushed *NA* and *EAF* slag, if compared with roundish *NA*. This result is in agreement with the works of Aitcin and Mehta [37] and Beshr et al [38], who pointed out the importance of coarse aggregate quality on the strength and elastic properties of high strength concretes. It is worth to note that the strength enhancement, often reported when studying *EAF* concretes, can be thus assigned not only to the shape of aggregates, but also to the nature of the slag itself. A better quality of the Interfacial Transition Zone (*ITZ)* zone was indeed observed in other experimental works in literature [9, 36].

Tensile strength enhancement was observed for concrete mixtures with low w/c and high cement dosage, using irregular shape aggregates: particularly, *EAF* concrete displayed an increase of + 32.5% on f_{ct}, whereas *CRU* concrete of + 14.5%, if compared to the *NAT* mixture. Also in this case a relevant contribution on tensile strength development of *EAF* concretes should be assigned to the angular shape of the slag, that causes a better adhesion between aggregate and matrix [9, 36].

Concerning concrete elastic properties, secant elastic modulus of *EAF* concretes is higher than conventional concretes' one, both in case of lower and higher strength mixtures. Conversely, concrete with crushed *NAs* exhibited the lowest elastic modulus, but not the lowest compressive strength. This result can be assigned to the chemical composition of the aggregates: crushed limestone *NA* might be more abundant in softer minerals than roundish *NA*. Additionally, it should be recalled that, at the load level used here (less than 33% of the ultimate load), the influence of the paste and its adherence with the aggregates is low on concrete elastic properties. Indeed, the elastic modulus of the aggregate (and consequently, its composition) is the more influencing parameter on E_c.

Table 3. Concretes properties.

	*NAT*300	*NAT*400	*CRU*300	*CRU*400	*EAF*300	*EAF*400
Fresh density (kg/m^3)	2257	2347	2343	2411	2563	2807
Slump (mm)	205	205	210	195	195	200
Hardened density (kg/m^3)	2307	2373	2371	2444	2668	2835
$f_{c,\ 7\ days}$ (MPa)	29.12	35.34	20.84	44.47	26.24	47.52
$f_{c,\ 28\ days}$ (MPa)	32.05	38.00	28.81	44.65	29.02	49.67
f_{ct} (MPa)	2.88	3.44	2.70	3.94	2.58	4.56
E_c (GPa)	36.32	42.69	33.02	35.26	39.23	45.69

4.2 Bond stress-slip relationships

4.2.1 Bond with ribbed bars

From pull-out tests, bond stress between reinforcing bars and concrete and stress-slip relationship can be obtained. Here the ultimate bond strength τ_U and the average bond strength τ_M are calculated for the specimens with ribbed bars, as recommended in [31]. The former is defined as the bond stress corresponding to the ultimate load (F_U), whereas the latter is calculated as the mean value of three bond stresses ($\tau_{0.01}$, $\tau_{0.10}$, $\tau_{1.00}$), corresponding to slip values of s = 0.01, 0.10 and

1.00 mm. The ultimate slip, s_u, which corresponds to the ultimate bond strength, is also measured. Additionally, normalized bond strength τ_U^* is calculated as the ultimate bond strength divided by the square root of the concrete compressive strength at 28 days. Table 4 lists the mean value and the standard deviation (*SD*) of the experimental bond characteristics, for each type of analyzed concrete. It is worth noting that the large majority of the tested specimens failed with a pull-out mode; only two specimens, made with EAF400 concrete failed due to splitting cracks occurrence. From Table 4, it can be observed that for the concretes prepared with high w/c ratio and low cement dosage, less differences were observed between the specimens made with the three mixtures, both in the ultimate and the average bond strength values. This can be assigned to the fact that pull-out failure is mainly governed by concrete compressive strength, which is very similar for the high w/c ratio specimens, being mostly affected by the similar quality of the cementitious matrix. Indeed, when analyzing the normalized bond strength τ_U^* of *NAT300*, *CRU300* and *EAF300* mixes, the mean of the three values is 2.06 MPa$^{0.5}$, with a standard deviation of 0.27 MPa$^{0.5}$. In the other mixtures having low w/c ratio, it can be observed that the concrete with *EAF* slag aggregates displayed higher ultimate and average bond strength than the conventional counterparts, both with roundish and crushed aggregates.

Table 4. Direct pull-out results (with ribbed bars).

specimen ID	$\tau_{0.01}$ (MPa)	$\tau_{0.10}$ (MPa)	$\tau_{1.00}$ (MPa)	τ_M (MPa)	τ_U (MPa)	τ_U^* (MPa$^{0.5}$)	F_U (kN)	s_U (mm)	failure type
NAT300	2.38	5.60	10.24	6.08	10.28	1.82	41.351	1.141	3PO
SD	*0.21*	*0.73*	*1.55*	*0.79*	*1.56*	*0.27*	*6.289*	*0.007*	
NAT400	4.13	8.36	17.35	9.94	17.50	2.84	70.369	0.848	3PO
SD	*1.41*	*3.45*	*0.56*	*1.39*	*0.54*	*0.09*	*2.163*	*0.103*	
CRU300	3.38	5.99	11.06	7.43	12.69	2.36	51.028	1.106	3PO
SD	*0.46*	*0.86*	*3.23*	*0.25*	*0.14*	*0.03*	*0.568*	*0.054*	
CRU400	5.77	10.63	19.23	11.87	19.04	2.85	76.549	1.213	3PO
SD	*0.33*	*1.06*	*0.35*	*0.35*	*0.89*	*0.13*	*3.586*	*0.088*	
EAF300	3.21	5.34	10.62	6.68	10.78	2.00	43.334	1.193	3PO
SD	*0.44*	*0.62*	*1.13*	*0.31*	*1.31*	*0.24*	*5.273*	*0.184*	
EAF400	4.99	8.86	23.59	12.27	24.72	3.51	99.402	1.245	1PO; 2S
SD	*0.39*	*1.48*	*1.18*	*0.82*	*0.30*	*0.04*	*1.206*	*0.573*	

It is significant that in two cases splitting failure mode was observed for *EAF400* mix: here the confinement was not sufficient to prevent splitting of concrete cover. Two/three radial cracks propagated through the entire cover, leading to a decrease of radial compressive stress, and when they reached the external surface, a marked drop of bond stress occurred. Comparing the normalized bond strength, the mean of the three values of *NAT400*, *CRU400* and *EAF400* mixes is 2.90 $MPa^{0.5}$, with a standard deviation of 0.39 $MPa^{0.5}$. A significant increase of this bond characteristic is obtained for the concrete with *EAF* slag (3.51 $MPa^{0.5}$), if compared to the other mixes, that instead are characterized by almost the same value (2.84 $MPa^{0.5}$).

Figures 2 and 3 show the global bond stress-slip curves (on the left) and a zoom of the pre-peak zone (on the right), for the specimens with ribbed bars: for each concrete, one curve only is plotted, being all the other similar. A threshold value between 3-4 MPa is observed, before slip evolution, in all the specimens. Looking at the stress-slip curves shown in Figure 2, a confirm of the above results can be obtained: the overall behavior of concretes prepared with high w/c ratio is similar for all the mixtures. Remarkable differences are instead observed in Figure 3, not only in the ascending branch of the curves (in the so-called stage 1 and 2 of bond development [39]), where the rib bearing bond mechanisms seems more pronounced in *EAF400* concrete. Indeed, also the frictional mechanism along the new sliding plane originated around the bar shearing off allowed the specimen to attain higher bond values. However, it should be recalled that, in this case, stress-slip curve of only one *EAF* concrete is shown in the graph, being the other specimens subject to splitting failure. Concerning *NAT400* and *CRU400* concretes, a similar ascending curve and post-peak response are visible. The most significant difference between the two curves is in the ultimate bond, which value is highly influenced by concrete compressive strength. Figure 4 shows the observed bond stress-slip curves of the two specimens failing due to splitting cracks occurrence: before splitting, the response is very similar to that of pull-out failure mode, then a sudden bond stress decrease is displayed.

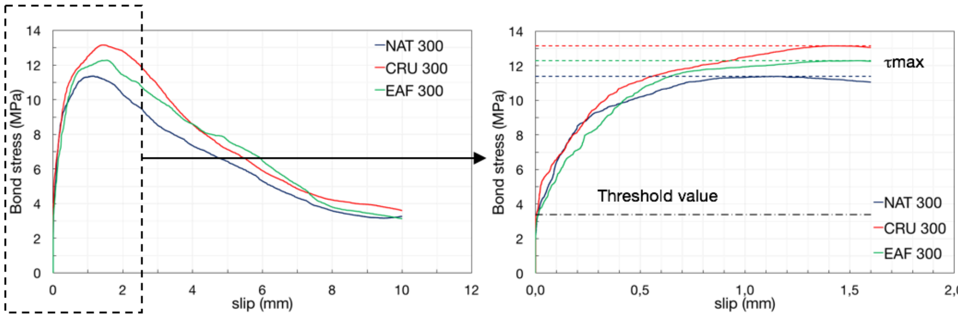

Figure 2. Experimental stress-slip curves (specimens with high w/c ratio and low cement content).

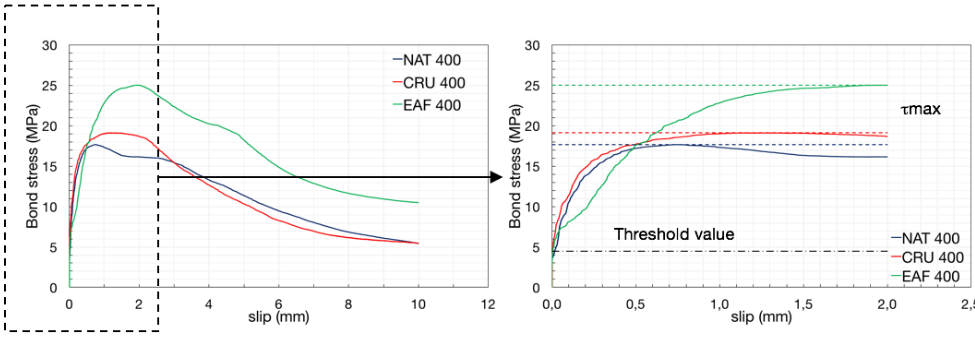

Figure 3. Experimental stress-slip curves (specimens with low w/c ratio and high cement content).
NB: For EAF 400 the curve refers to the only specimen which displayed a pull-out failure.

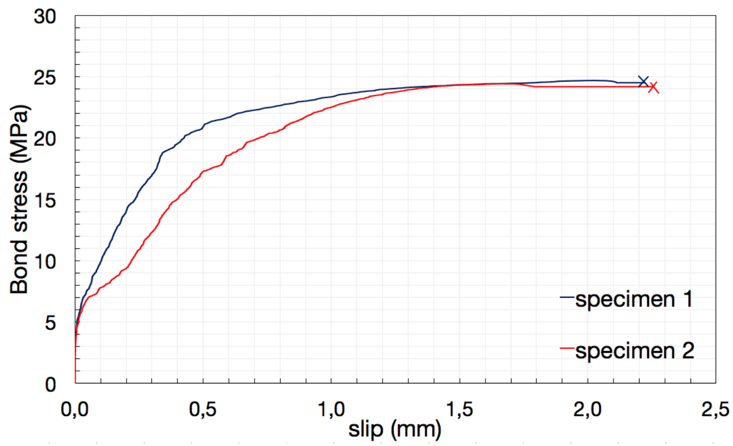

Figure 4. Experimental stress-slip curves of *EAF400* specimens – splitting failure mode.

4.2.2 Bond with plain bars

All the specimens with plain bars failed due to pull-out failure mode. According to the experimental stress-slip response, in the chemical adhesion mechanism branch, a rapid rise of the stress is observed, at very low values of slippage, in the same way that could be appreciated in the ribbed bars stress-slip curves (values below 4 MPa in high w/c ration and below 8MPa in low w/c ratios). Once the chemical adhesion is broken, the bond stress drops quickly and the further resistance is provided mainly by friction. Accordingly, the descending part of the stress-slip curve is characterized by a softening branch, due to the degradation of the frictional component of bond [40], and by a horizontal branch, corresponding to the ultimate frictional resistance. Ultimate bond strength τ_U at the ultimate load (F_U), purely frictional bond strength τ_f, evaluated in the post-peak softening branch where the slope ($d\tau/ds$) is null, and the normalized bond strength τ_U^* are listed in Table 5, for each type of concrete. Standard deviation of the results is also reported (*SD*).

The ultimate bond strength is sensibly lower than in specimens including ribbed bars: transfer capacities are low and the deformation of bars during the test is largely below steel elastic limit. For high w/c ratio concretes, *EAF300* mix attained the highest ultimate bond resistance, whereas the frictional bond seemed to offer similar resistance for all the type of specimens. Conversely, for the low w/c concretes, no significant strength differences were experienced by the mixes including crushed aggregates (*CRU400* and *EAF400*), which displayed an ultimate strength enhancement of about + 48% than *NAT400* conglomerate. Also the frictional bond value is proportionally higher than in the reference mixture. It can be noted that, in the case of bond with plain bars, higher dispersion of results is obtained than with ribbed ones. Indeed, the mean standard deviation of the analyzed bond parameters is about 22% for plain bars; this value decreases around 6% for ribbed bars bond. This may be due to the variability in the steel surface roughness. Additionally, the slip at the bond peak value is relatively low for smooth bars as compared to that observed for deformed bars.

Table 5. Direct pull-out results (with plain bars).

specimen ID	τ_U (MPa)	τ_U^* (MPa$^{0.5}$)	τ_f (MPa)	F_U (kN)	s_U (mm)	failure type
NAT300	1.21	0.21	0.69	4.852	0.08	3PO
SD	*0.41*	*0.08*	*0.27*	*1.658*	*0.02*	
NAT400	1.58	0.26	0.84	6.363	0.07	3PO
SD	*0.01*	*0.01*	*0.04*	*0.047*	*0.02*	
CRU300	1.07	0.20	0.64	4.283	0.10	3PO
SD	*0.13*	*0.02*	*0.06*	*0.531*	*0.03*	
CRU400	2.35	0.35	1.30	9.450	0.45	3PO
SD	*0.31*	*0.05*	*0.39*	*1.273*	*0.21*	
EAF300	1.46	0.27	0.73	5.858	0.15	3PO

SD	*0.82*	*0.15*	*0.12*	*3.308*	*0.02*	
EAF400	2.34	0.33	1.15	9.411	0.26	3PO
SD	*0.38*	*0.05*	*0.61*	*1.542*	*0.01*	

4.3 Comparison of experimental results with predicting equations

Many authors proposed predicting equation for the assessment of the bond strength between concrete and ribbed bars, both for pull-out and splitting failure, in case of monotonic loading. Particularly, idealized stress-slip curves can describe the experimental behavior of bond between concrete and ribbed bars. Most of the existing formulations include, as relevant parameter, concrete compressive strength f_c, concrete cover c, steel bar diameter d and the embedment length l_b. Some of them include also the confinement influence, which is considered as one of the main parameters affecting the failure mode.

Oragun et al. [41] proposed an empirical formulation (Eq. 2), based on a non-linear regression analysis of tests carried out on beam-specimens with unconfined lap splices. The equation was derived using a dataset having mostly *c/d* values less than 2.5; specimens failing due to splitting after steel yielding were not taken into account in the regression. Stresses are expressed in (Psi).

$$\tau_u = \left[1.22 + 3.23 \cdot \left(\frac{c}{d}\right) + 53 \cdot \left(\frac{d}{l_b}\right)\right] \cdot \sqrt{f_c} \tag{2}$$

Kemp [42] proposed a prediction equation (Eq. 3) obtained through a multiple linear regression analysis, derived on a total of 157 stub cantilever specimens. The influence of clear cover, bar spacing, stirrups, and dowel forces were studied in this research. Stresses are expressed in (Psi).

$$\tau_u = 232 + 2.716 \cdot \left(\frac{c}{d}\right) \cdot \sqrt{f_c} \tag{3}$$

Chapman and Shah [43] conducted an experimental investigation for the assessment of bond stress at early age of concrete maturation. They developed an empirical formulation based on pull-out specimens (Eq. 4), which is very conservative in the prediction of matured concrete specimens, also according to the same authors. They did not distinguish between pull-out, splitting or steel bar yielding failure, and the stresses in the formulation are expressed in (Psi).

$$\tau_u = \left[3.5 + 3.4 \cdot \left(\frac{c}{d}\right) + 57 \cdot \left(\frac{d}{l_b}\right)\right] \cdot \sqrt{f_c} \tag{4}$$

Al-Jahdali et al. [44] proposed an expression (Eq. 5) for bond strength estimation, with unites expressed in the S.I. system, based on an experimental campaign on

36 pull-out specimens. Also in this case the authors did not distinguish between the possible failure modes, i.e. splitting, pull-out, tensile concrete fracture and steel yielding.

$$\tau_u = \left[-0.879 + 0.324 \cdot \left(\frac{c}{d}\right) + 5.79 \cdot \left(\frac{d}{l_b}\right)\right] \cdot \sqrt{f_c} \qquad (5)$$

Recently Aslani and Nejadi [45] proposed an empirical formulation (Eq. 6), derived from tests conducted on both pull-out and beam-specimens made with self-compacting concrete, collected in literature. They did not distinguish between possible failure modes, and units are expressed in the S.I. system.

$$\tau_u = \left[0.672 \cdot \left(\frac{c}{d}\right)^{0.6} + 4.8 \cdot \left(\frac{d}{l_b}\right)\right] \cdot f_c^{0.55} \qquad (6)$$

Also some Code previsions are currently available for bond strength estimation: particularly, the *fib* Model Code 2010 [46] provides two equations, for splitting without transverse reinforcement (Eq. 7) and for pull-out failure (Eq. 8), respectively. MC2010 makes a distinction between good and all other bond conditions: the former is considered when the bar has an inclination of 45-90° with respect to the horizontal, during concrete casting. The latter is instead used when the casting position of the bars has an inclination less than 45° to the horizontal, and reinforcement are located up to 250 mm from the bottom or at least 300 mm from the top of concrete layer. Here the equations for "all other bond conditions" are reported, according to bars location during casting operations. It should be recalled that, in this case, both c_{min} and c_{max} correspond to 4.5, being respectively the minimum and maximum concrete cover in the tested element.

$$\tau_{u,split} = 0.7 \cdot 6.5 \cdot \left(\frac{f_{cm}}{25}\right)^{0.25} \cdot \left(\frac{25}{d}\right)^{0.2} \cdot \left[\left(\frac{c_{min}}{d}\right)^{0.33} \cdot \left(\frac{c_{max}}{c_{min}}\right)^{0.1}\right] \qquad (7)$$

$$\tau_{u,pull-out} = 1.25 \cdot \sqrt{f_c} \qquad (8)$$

Since the tested specimens in this work have short embedment length (l_b = 5d), the experimental bond–slip curve can be used for a comparison with the local stress–slip law proposed by MC2010. The Bertero-Popov-Eligehausen (*BPE)* model (Figure 5), initially proposed by Eligehausen [32] and then adopted in the same Code, can be used for the evaluation of the bond stress at the correspondent slip value. The parameters for defining the mean bond stress-slip relationship of deformed bars can be found in Table 6.1-1 of the MC2010. For pull-out failure and "all other bond conditions", the value of α coefficient is assumed as 0.4, s_u is 1.8 mm, s_2 is 3.6 mm and s_f is the clear distance between the ribs, equal to 10 mm in this case. The value of ultimate bond resistance is given by the ultimate pull-out strength (Eq. 8), and frictional strength τ_f is about $0.4 \cdot \tau_{u,pull-out}$.

$\tau = \tau_u \cdot (\frac{s}{s_u})^\alpha$ For $0 \leq s \leq s_u$

$\tau = \tau_u$ For $s_u \leq s \leq s_2$

$\tau = \tau_u - (\tau_u - \tau_f) \cdot (s - s_2)/(s_f - s_2)$ For $s_2 \leq s \leq s_f$

$\tau = \tau_f$ For $s_f < s$

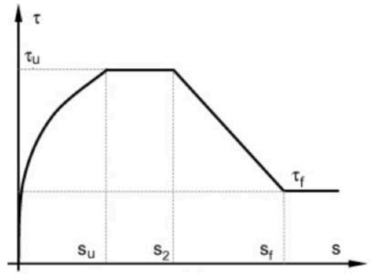

Figure 5. *BPE* model [32] adopted in the *fib* MC2010 for bond stresses estimation between concrete and reinforcing bars (monotonic loading – deformed bars).

Concerning instead the bond between concrete and plain bars, the current literature does not offer many contributions about this issue [47]. The *fib* MC2010 assumes a model constituted by a first monomial ascending branch (Eq. 9), and then a second constant one where $\tau_u = \tau_f$ for $s > s_u$.

$$\tau = \tau_u \cdot (\frac{s}{s_u})^\alpha \quad (9)$$

The value of the coefficient α is equal to 0.5, and s_u is 0.1 mm for hot rolled bars with "all other bond conditions", whereas the value of $\tau_u = 0.15 \cdot \sqrt{f_c}$.

Figure 6 shows the estimated vs. the experimental ultimate bond stress of the specimens analyzed in this work, using the above formula. It is worth to recall that experimental materials properties have been used to compute the theoretical values of analyzed formulations. Particularly, the value of f_c obtained using 100x200 mm cylindrical specimens has been used, without using any conversion factors to assess the strength on 150x300 mm specimens (negligible: error experimentally assessed as 2%). A poor correlation between the experimental results and the theoretical values is obtained using all the provisional formula. It is indeed worth to note that most of these formula "converge" to a range of constant values, because of few influencing parameters (concrete compressive strength, concrete cover and bar diameter), which are also not significantly varying in the present experimental campaign. Additionally, some of the previous formula (Eq. 2 and 3) were derived on a set of beam-type specimens only, and this contributed to the underestimation of the ultimate bond strength. The only formulation which provided largely unconservative estimates of the ultimate bond strength is Eq. 6, which was derived for SCC concretes, which exhibited even better bond than ordinary vibrated concretes in some cases in literature.

Concerning the prediction of the MC2010 model, a comparison between estimated and experimental bond strength was done. Eq. 7 has been applied to specimens that displayed splitting failure, and Eq. 8 to the ones failing with a pull-out mode. The results obtained with both equations are highly conservative, especially ones concerning pull-out failure mode.

It is worth to mention that similar values can be obtained applying both Eq. 3 (Kemp 1986) and Eq.7 (MC2010 for pull-out failure). Particularly, at low values of τ_u, the prediction of the two models is almost the same. Instead, at higher values of τ_u, the prediction of MC2010 gives higher theoretical values than the Kemp formulation.

Concerning instead the prediction of the slip characteristic values in MC2010 (Figure 5), looking at the results in Table 4, it is possible to observe a well estimation of the slip at maximum load s_{max}. The frictional bond strength, evaluated at a slip value equal to the clear distance between two successive ribs, is underestimated in case of high w/c concretes; on the contrary, a better fit is observed for the low w/c ratio ones, particularly for *NAT400* and *CRU400* specimens.

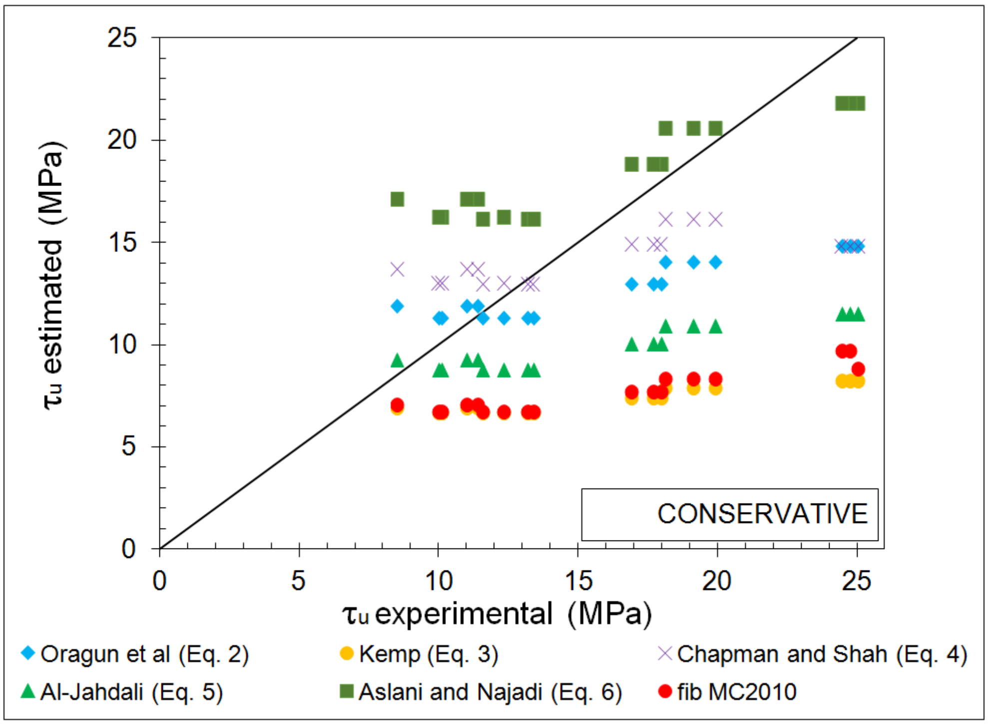

Figure 6. Estimated vs. experimental ultimate bond strength for deformed bars.

A conservative prediction of the MC2010 equation (Eq. 9) for bond between concrete and plain bars is observed: Figure 7 shows the comparison between estimated and experimental ultimate bond strength.

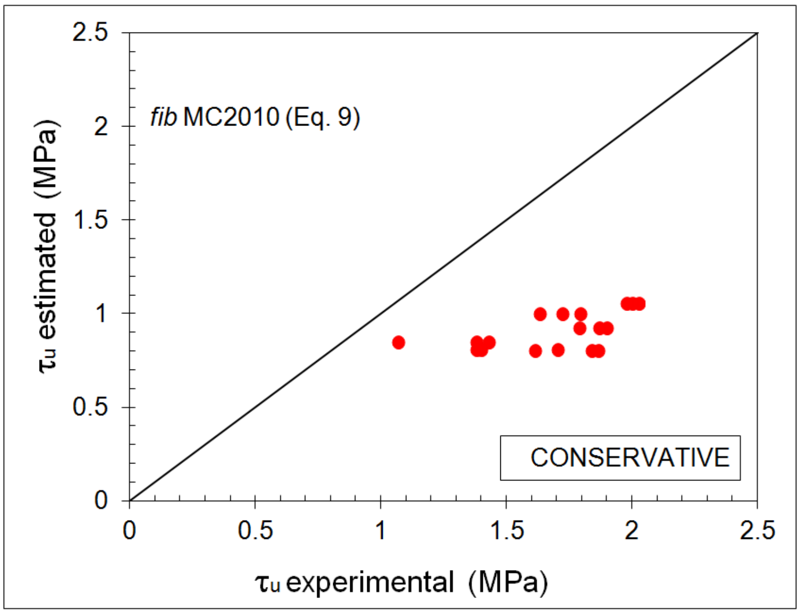

Figure 7. Estimated vs. experimental ultimate bond strength for smooth bars.

5. Conclusions

This works deals with an important aspect of structural application of electric arc furnace slag, namely the bond between concrete and steel reinforcement bars, about which no works were carried out in literature up to now. A future development of this research would be the assess of bond characteristics using the beam end test. According to the experimental results obtained in this work, the following conclusions can be drawn:

- The use of *EAF* slag as coarse aggregate allows compressive strength enhancement up to 30% when it is used as substitution of natural roundish aggregate, and up to 17.5% when it replaces crushed natural ones. This behavior can be observed in concretes prepared with low w/c ratio, where ultimate strength is not affected by poor cementitious matrix quality. Strength gain can be assigned both to slag shape and texture, and to its enhanced mechanical properties and chemical composition, which improves the quality of the *ITZ*, as observed also in other literature works;

- Bond strength between concrete and ribbed steel bars (mean, ultimate and residual frictional) is higher when crushed aggregates are used, referring to low w/c concretes. The highest bond strength is observed in specimens including *EAF* slag, with an increase of + 41% and + 30% in the peak stress, respectively on *NAT* and *CRU* mixture. Concerning concretes manufactured with high w/c ratio, few differences are observed between the tested mixtures;
- Concerning bond with plain bars, higher variability in the results are obtained than with ribbed ones. Also in this case a substantial increase in the ultimate strength is displayed by mixtures with crushed aggregates if compared to *NAT* mixture;
- The existing predicting equations for ultimate bond strength prediction with ribbed bars are typically conservative for (relatively) high strength concretes, whereas they fit better for low strength concretes. The equations proposed by Kempt and *fib MC2010* are the more conservative;
- Concerning bond between concrete and plain bars, conservative values have been obtained using the *fib MC2010* equation. In this case differences obtained for high and low w/c ratios are quite similar.

Acknowledgments

This work is supported by the Spanish Ministry MINECO and FEDER Funds for financial support through Project BlueCons: BIA2014-55576-C2-2-R. Also the authors would to express their gratitude to the Vice-Rectorate of Investigation of the University of the Basque Country for grant PIF 2013, the grant for mobility of researchers 2015 and, likewise, to the Basque Government for financial support to Research Group IT781-13. The authors would like also to thank Zerocento S.r.l. for providing the EAF slag, and to Francesco Galdeman for his help during the experimental campaign.

Compliance with Ethical Standards

Conflict of Interest: The authors declare that they have no conflict of interest.

References

[1] Douglas E, Bilodeau A, Brandstetr J, Malhotra VM (1991) Alkali activated ground granulated blast-furnace slag concrete. Preliminary investigation. Cem Concr Res 21(1): 101-108. doi: 10.1016/0008-8846(91)90036-H.

[2] Jelidi A, Bouslama S (2015) Use effects of blast furnace slag aggregates in hydraulic concrete. Mater Struct 48(11): 3627-3633. doi: 10.1617/s11527-014-0427-z.

[3] Reddy AS, Pradhan RK, Chandra S (2006) Utilization of basic oxygen furnace (BOF) slag in the production of a hydraulic cement binder. Int J Miner Process 79(2): 98-105.

[4] Manso JM, Polanco JA, Losañez M, González JJ (2006) Durability of concrete made with EAF slag as aggregate. Cem Concr Comp 28: 528 - 534.

[5] Papayianni I, Anastasiou E (2010) Production of high-strength concrete using high volume of industrial by-products. Constr Build Mater 24: 1412 – 1417.

[6] Pellegrino C, Cavagnis P, Faleschini F, Brunelli K (2013) Properties of concretes with black/oxidizing electric arc furnace slag aggregate. Cem Concr Comp 37: 232-240.

[7] Pasetto M, Baldo N (2012) Performance comparative analysis of stone mastic asphalt with electric arc furnace steel slag: a laboratory evaluation. Mater Struct 45-3: 411-424.

[8] Faleschini F, De Marzi P, Pellegrino C (2014) Recycled concrete containing EAF slag: environmental assessment through LCA. Eur J Environ Civ Eng 18-9: 1009-1024.

[9] Arribas I, Santamaría A, Ruiz E, Ortega-López V, Manso JM (2015) Electric arc furnace slag and its use in hydraulic concrete. Constr Build Mater 90: 68-79.

[10] Pellegrino C, Gaddo V (2009) Mechanical and durability characteristics of concrete containing EAF slag as aggregate. Cem Concr Comp 31: 663-671.

[11] Faleschini F, Fernández-Ruíz MA, Zanini MA, Brunelli K, Pellegrino C (2015) High performance concrete with electric arc furnace slag as aggregate: Mechanical and durability properties. Constr Build Mater 101: 113-121.

[12] Polanco JA, Manso JM, Setién J, González JJ (2011) Strength and Durability of Concrete Made with Electric Steelmaking Slag. ACI Mater J 108: 196-203.

[13] Manso JM, Polanco JA, Losañez M, González JJ (2006) Durability of concrete made with EAF slag as aggregate. Cem Concr Comp 28: 528 - 534.

[14] Arribas I, San José J.T., Vegas I.J., Hurtado J.A., Chica J.A. (2010) Application of steel slag concrete in the foundation slab and basement wall of the Labein- Tecnalia Kubik building. 6th European Slag Conference, EUROSLAG pub Nº5. Madrid: UNESID.

[15] Pellegrino C, Faleschini F (2013) Experimental behavior of reinforced concrete beams with electric arc furnace slag aggregate. ACI Mater J 110-2: 197-205.

[16] Kim A-W, Kim Y-S, Lee J-M, Kim K-H (2013) Structural performance of spirally confined concrete with EAF oxidizing slag aggregate. Eur J Environ Civ Eng 17(8): 654-674.

[17] Abrams DA (1913) Test of Bond Between Concrete and Steel. Bulletin no. 71, Engineering Experiment Station, University of Illinois, Urbana, p 105.

[18] Clark AP (1950) Bond of concrete reinforcing bars. ACI J 46(3):161–184.

[19] ACI Committee 408 (1966) Bond Stress – The State of the Art, ACI J, Proceeding 63(11): 1161-1188.
[20] Cairns J, Jones K (1995) Influence of rib geometry on strength of lapped joints: an experimental and analytical study. Mag Concr Res 47(172):253–262
[21] Gambarova PG, Rosati GP (1997) Bond and splitting in bar pull-out: behavioural laws and concrete-cover role. Mag Concr Res 48(6): 99–110.
[22] Hamad BS, Itani MS (1998) Bond strength of reinforcement in high-performance concrete: the role of silica fume, casting position, and superplasticizer dosage. ACI Mater J 95(5):499–511.
[23] Dancygier A and Katz A (2010) Bond between deformed reinforcement and normal and high-strength concrete with and without fibers. Mater Struct 43(2): 839–856.
[24] Metelli G, Plizzari GA (2014) Influence of the relative rib area on bond behavior. Mag Concr Res 66(6): 277-294.
[25] Pecce M, Ceroni F, Bibbò FA, Acierno S (2015) Steel-concrete bond behaviour of light-weight concrete with expanded polystyrene (EPS). Mater Struct 48(1): 139-152.
[26] Xiao J, Falkner H (2007) Bond behaviour between recycled aggregate concrete and steel rebars. Constr Build Mater 21:395–401.
[27] Seara-Paz S, González-Fonteboa B, Eiras-López J, Herrador MF (2014) Bond behavior between steel reinforcement and recycled concrete. Mater Struct 47: 323-334.
[28] Guerra M, Ceia F, de Brito J, Júlio E (2014) Anchorage of steel rebars to recycled aggregates concrete. Constr Build Mater 72: 113-123.
[29] Prince MJR, Singh B (2015) Bond strength of deformed steel bars in high-strength recycled aggregate concrete. Mater Struct 48: 3913-3928.
[30] *fib* (2014) Task Group 4.5: Bond Models, Convenor J. Cairns. Bond and anchorage of embedded reinforcement: Background to the *fib* Model Code for Concrete Structures 2010 – fib, Lausanne, Switzerland.
[31] RILEM/CEB/FIP (1978) Bond test for reinforcing steel: 2. Pullout Test, Recommendation RC 6.
[32] Eligehausen R, Popov EP, Bertero VV (1983) Local bond stress–slip relationships of deformed bars under generalized excitations. University of California, report no. UCB/EERC-83/23.
[33] Daoud A, Lorrain M, Elgonnounil M (2002) Resistance à l'arrachement d'armatures ancrées dans du béton autoplaçant. Mater Constr 35: 395–401.
[34] Valcuende M, Parra C (2009) Bond behaviour of reinforcement in self-compacting concretes. Constr Build Mater 23: 162–170.
[35] RILEM (1982) Bond test for reinforcement steel. 1. Beam test, recommendation RC 5.
[36] Faleschini F, Brunelli K, Zanini MA, Dabalà M, Pellegrino C (2016) Electric Arc Furnace as Coarse Recycled Aggregate for Concrete Production. J Sustain Metall 2-1: 44-50
[37] Aitcin PC, Mehta PK (1990) Effect of coarse-aggregate characteristics on mechanical properties of high-strength concrete. ACI Mater J 87(2): 103-107.

[38] Beshr H, Almusallam AA, Maslehuddin M (2003) Effect of coarse aggregate quality on the mechanical properties of high strength concrete. Constr Build Mater 17(2): 97-103.

[39] den Uijl JA, Bigaj AJ (1996) A bond model for ribbed bars based on concrete confinement. HERON 41(3), ISSN: 0046-7316.

[40] Stoker MF, Sozen MA (1970) Investigation of prestressed reinforced concrete for highway bridges. Part V: bond characteristics of prestressing strand. University of Illinois at Urbana-Champaign Bulletin 503.

[41] Oragun CO, Jirsa JO, Breen JE (1977) A reevaluation of test data on development length and splices. ACI J 74(3): 114–122.

[42] Kemp EL (1986) Bond in reinforced concrete: behavior and design criteria. ACI J 83(7): 50-57.

[43] Chapman RA, Shah SP (1987) Early-age bond strength in reinforced concrete. ACI Mater J 84(6): 501–510.

[44] Al-Jahdali FA, Wafa FF, Shihata SA (1994) Development Length for Straight Deformed Bars in High-strength Concrete, ACI SP-149: 507–522.

[45] Aslani F, Nejadi S (2012) Bond behavior of reinforcement in conventional and selfcompacting concrete, Adv. Struct. Eng. 15 (12) 2033.

[46] *fib* Model Code 2010 (2012) Final Draft, Fédération Internationale du Béton *fib* - International Federation for Structural Concrete.

[47] Verderame GM, De Carlo G, Ricci P, Fabbrocino G (2009) Cyclic bond behaviour of plain bars. Part II: Analytical investigation. Constr Build Mater 23: 3512-3522.